4-8-2019

Oxygen and Hydrogen isotopes in human hair and tap water: Modeling relationships in a Modern Mexican Population

Chelsey A. Juarez
Department of Anthropology California State University Fresno, chelseyjuarez@mail.fresnostate.edu

Robin Ramey
Fairfax County Park Authority

David T. Flaherty
Department of Molecular Biomedical Sciences North Carolina State University

Belinda Akpa
Department of Molecular Biomedical Sciences North Carolina State University, bsakpa@ncsu.edu

Oxygen and Hydrogen Isotopes in Human Hair and Tap Water: Modeling Relationships in a Modern Mexican Population

Chelsey A. Juarez,[1]* Robin Ramey,[2] David T. Flaherty,[3] and Belinda S. Akpa[3]*

[1]Department of Anthropology, California State University, Fresno, Fresno, California, USA.

[2]Fairfax County Park Authority, Virginia, USA.

[3]Department of Molecular Biomedical Sciences, North Carolina State University, Raleigh, North Carolina, USA.

*Correspondence to:

Chelsey Juarez, Department of Anthropology, California State University, Fresno, Peters Business Building, Room 385, 5245 North Backer Ave. M/S PB16, Fresno, CA 93740-8001 USA. E-mail: chelseyjuarez@mail.fresnostate.edu.

Belinda S. Akpa, Department of Molecular Biomedical Sciences, North Carolina State University, 1060 William Moore Dr., Raleigh, NC 27604 USA. E-mail: bsakpa@ncsu.edu.

Short Title: Δ2H and Δ18O Isotopes in Mexican Tap Water and Hair

KEY WORDS: Δ2H, Δ18O, MEXICO, TAP WATER, HAIR

Abstract

This study investigates the relationship between O and H isotopes in samples of Mexican hair and drinking water. The purpose of this study was twofold. First, we wanted to quantify the relationship between isotopes in Mexican hair and tap water to understand the impact of water stress and differing socioeconomic status on accurate predictions of drinking water. Second, we wanted to determine whether currently existing semi mechanistic models could accurately represent the relationship between hair and tap water. For this study, we used a subset of paired (N = 62) human hair and (N = 76) tap water samples. Isotope values in tap water spanned a range from –11.4 ‰ to –4.3 ‰ and –79.1 ‰ to –22.5 ‰ for $\delta^{18}O$ and $\delta^{2}H$, respectively. Isotope values in hair ranged from +9.5 ‰ to +16.1 ‰ and –90.8 ‰ to –53.7 ‰ for $\delta^{18}O$ and $\delta^{2}H$, respectively. The most depleted $\delta^{18}O$ and $\delta^{2}H$ hair values came from individuals in the state of Morelos. For our modern Mexican population, positive correlations between isotopes in hair and water were not significant, with correlation coefficients of r = 0.61 (p = 0.05) and r = 0.60 (p = 0.06) for ^{18}O and ^{2}H respectively. Error-in-variables regression yielded linear fits that were somewhat better for ^{2}H relative to ^{18}O: $\delta^{18}O_{h} = 0.183\ [\pm 0.132]\ \delta^{18}O_{tw} + 15.7\ [\pm 0.9]$ ‰ ($r^2 = 0.23$); $\delta^{2}H_{h} = 0.181\ [\pm 0.076]\ \delta^{2}H_{tw} - 64.0\ [\pm 3.0]$ ‰ ($r^2 = 0.34$). In short, data from this Mexican population do not exhibit the strong relationships between isotope values of ^{18}O and ^{2}H in tap water and hair that have been characteristic of other populations studied to date. Given the economic stratification of this region and the poor correlation between hair and water samples, we chose to consider the possibility that *l* – the fraction of the diet derived from local sources –and f_s – the fraction of non-exchangeable H in keratin that was fixed *in vivo*–are local, rather than global, parameters for this population. We estimated a different value of *l* and f_s for each location. Given the anticipated importance of the non-local dietary contribution, we treated the isotopic content of non-local

food and the offset parameters for predicting isotopes in locally derived food as tuning parameters and compared the results with the parameters based on the American supermarket diet. We found that, although O and H isotopes in water and hair maintain similar geographic distributions, O and H isotopes in tap water explain only a small part of the variation observed in hair samples. In comparison to the standard American supermarket diet, the Mexican estimates for non-local diet and local diet offsets predict regional distributions of l and f_s that cleanly segregate urban areas from rural towns.

In the last fifteen years, there has been growing interest in the application of water isotope analysis to provenience and migratory behavior for populations of forensic significance. Border deaths along the U.S Mexico border – as well as the deaths of undocumented immigrants within the greater United States – present an opportunity where discriminating region of origin information or migration behavior would be particularly useful (Ross et al., 2016). Deceased, undocumented border-crossers from Latin America offer unique challenges for the successful application of O and H isotopes in water – due in part to issues of drinking water insecurity and dramatic differences in socioeconomic status (SES) in these regions (Sosa-rodriguez, 2012).

In large part, the focus on geolocation in a forensic context has been on human keratin and water relationships in locations where populations use available tap water for drinking (Bowen et al., 2005, 2009; O'Brien and Wooller, 2007; Ehleringer et al., 2008; Meier-Augenstein and Fraser, 2008; Podlesak et al., 2008; Meier-Augenstein and Kemp, 2010; Thompson et al., 2010). Unlike U.S populations, Mexican populations rely heavily on bottle water that may or may not be generated from their local water supply. Given the complex relationship between Mexican populations and drinking water, this study investigates the relationship between O and H isotopes in samples of Mexican hair and tap water and their role in provenience analysis. We explore the relationships between paired tap water and hair samples of known Mexican origin from Central and Southern Mexico and interpret these relationships in the light of water insecurity and extreme socioeconomic stratification. In doing so, we reconsider the underlying assumptions of semi-mechanistic models that aim to predict isotopes in hair based on those in drinking water and food consumed.

Background

Geographic Isotope Variations in Precipitation Impact Isotopic Content of Human Tissues. Precipitation gradients in ^{18}O and ^{2}H isotopes impact plant and animal tissues as well as natural drinking water reservoirs. Oxygen and hydrogen isotopes in precipitation vary predictably with geography. Lower isotope values are found at higher altitude and latitudes and higher isotope values are associated with coastal regions and low latitudes (Bowen et al., 2007). It is well established that drinking water and food water apply the primary controls on hair ^{2}H and ^{18}O isotopes (Hobson et al., 1999; Sharp et al., 2003; O'Brien and Wooller, 2007; Ehleringer et al., 2008; Podlesak et al., 2008). Approximately one third of the H isotope content of hair is derived from drinking water; the remainder comes from food (Sharp et al., 2003). The oxygen atoms in human hair are determined by complete isotopic exchange with gut water during hydrolysis of dietary protein. Body water and gut water pools are suggested to be similar in composition, with the major constituents of body water deriving from drinking water, water content of food, and oxygen in food (Ehleringer et al., 2008; Podlesak et al., 2008, 2012; Chesson et al., 2010). O and H isotopes in hair are enriched in comparison to diet or respiration inputs but reflect gradients analogous to those evident in the environment from which these inputs are derived. As tissues remodel over time, they can thus record evidence of migration by revealing associated shifts in food and water sources. This is particularly true for a fast-growing tissue like hair, which rapidly acclimatizes to food and water intake. Hair grows approximately 0.3 mm per day and has an acclimation period of approximately one month (Williams et al., 2011). Thus, hair provides data on sustained location, as well as migration.

In Mexico, Water Stress Complicates Access to Local Drinking Water. Use of relationships between O and H isotopes in hair and water to infer region of residence would seem appropriate for Mexico, as the states show significant climatic and elevation differences.

However, Mexico has a long history of water stress that complicates access to local water. Water scarcity refers to the abundance or lack of water supply, and water stress refers to the inability to meet the human need for water (Spring, 2014). This challenge dates back to the 1930s when hydraulic engineers began detecting aquifer depletion (Wolfe, 2017). Once Mexican states began to institute municipal water plans in the early 1900s, uneven development, poor water sanitation, epidemics, seismic damage, and deficiencies in municipal repairs led to disparities in water stress and or water scarcity among states (Ayala and O'Rourke, 1989; Borroto and Martinez-Piedra, 2000; Davis, 2005; Armienta and Segovia, 2008; Bundschuh et al., 2012; Sosa-rodriguez, 2012; Espinosa-García et al., 2015; Arcega-Cabrera et al., 2017; Rodríguez-Tapia et al., 2017). Furthermore, water-borne diseases such as cholera, amebiasis, and cysticercosis, and high levels of dental fluorosis have intermittently plagued the municipal water system dissolving public trust in water safety (Russel and Elvove, 1962; Borroto and Martinez-Piedra, 2000; Soto-Rojas et al., 2004; Sepúlveda et al., 2006; Armienta and Segovia, 2008; Bundschuh et al., 2012; Greene, 2014; Montero-Contreras, 2016; Hernandez-Cortazar et al., 2017).

Depending on their state of residence, between 80% and 100% of Mexicans report using bottle water as their only source of drinking water (WHO/UNICEF Joint Monitoring Programme, 2017). Expenditure on bottle water can be more than 14% of monthly income per household, and reports of contamination in bottled waters keeps the market fluid (Gutieŕrez et al., 2012). While beverage suppliers may draw their water from local sources, that is often not the case. There are four major companies in the Mexican bottled water industry (Coca-Cola/FEMSA, Nestle, PepsiCo, and Danone) that have approximately 80% of the overall bottled water market share, and over 6000 small companies that make up the remaining 20% market share (Greene, 2014). Pinpointing water sources for the large suppliers is complex. For example, Coca-Cola/FEMSA has 17 bottling plants in Mexico, and each plant supplies its own region (Pani, 2017). In contrast, water from the Chiapas Coca-Cola plant is distributed more widely and represents ~5-7% of bottle water beverages in the country. All the large suppliers have plants in the Valley of Toluca in the State of Mexico, and they draw from similar water sources. Bottled water is not strictly regulated in Mexico, and both small and large companies draw water from multiple sources including aquifers, groundwater, rainwater, and river water. For example, since 2000, Coca-Cola has used water from 19 different aquifers and 15 different rivers (Franco et al., 2015). In summary, drinking water in Mexico can come from any number of different sources that are not necessarily local to an individual's place of residence.

The Role of Isoscapes in Provenience Analysis. Provenience studies using geographic patterns of O and H isotopes in drinking water and human tissues require: 1) the collection of large known-sample databases for drinking water and hair, and 2) knowledge about isotopes in dietary sources of protein. In forensic analysis of provenience, isoscapes –large geospatial models of isotope distributions and predictions of isotope values based on these distributions – have become common place (Hobson et al., 1999; Bowen et al., 2007; Ehleringer et al., 2008, 2010; Wassenaar et al., 2009; Bataille and Bowen, 2012; Warner et al., 2018). Human tissue samples representing living populations often do not have ideal spatial distributions; however, the predictive power of isoscapes function as a way to synthesize isotope distributions over geography in spite of these inconsistencies. This feature of isoscapes is both a strength and a weakness since reliable predictions of isotope geographical distributions require a reasonable spatial distribution of baseline data and constant attention to modeling methodologies (Ehleringer et al., 2010; West et al., 2010; Chesson et al., 2018). Moreover, isoscapes used for human provenience and based on human tissues must also be sensitive to the real time changes in isotope distributions resulting from social, environmental, and economic change. If based on well-sampled isotope signatures from water and tissues, isoscapes are a valuable reference for provenience studies of human remains. Where tissue isoscapes are absent or inadequately sampled, mathematical models hold significant appeal as a means of predicting the missing tissue data.

Predicting Isotopes in Hair from Those in Water Using Semi-Mechanistic Models. In 2008, Ehleringer and colleagues codified the relationships between food and water consumption and stable isotope signatures of hair in the form of a semi-mechanistic model. Figure 1 is a pathway diagram showing, conceptually, how O and H isotopes of hair can be predicted from the key inputs of food and water. Those location-dependent primary model inputs are denoted by double-lined boundaries, as is the input of oxygen, which enters the body via breathing. All other compartments in the diagram represent intermediate calculations used to fractionate isotopes into the primary output, which is the hair. The population of interest in this study was contemporary residents of the continental United States, who were presumed to be consuming municipally supplied tap water and a diet of supermarket foods. The water could thus be expected to represent a ‘local’ isotopic input, while the food – a product mainly of large-scale industrial agriculture and far-reaching distribution channels – could be treated as homogenous and common to all the sampled populations. Thus, practically, the Ehleringer et al. (2008) model presumes a linear relationship between O and H isotopes of hair and drinking water. A simple regression on isotopic data indicated this assumption to be valid for stable isotopes in paired hair and tap water data obtained for residents of the United States, leading the authors to posit that drinking water accounts for a substantial part of the geographical variation of O and H isotopes in hair samples.

The Ehleringer et al. (2008) model has 28 parameters, many of which are at least partly constrained by prior empirical research. However, several parameters are either poorly constrained or likely to be subject to inter-population variability of sufficient interest to warrant tuning to empirical data. In modeling the relationship between O and H isotopes in hair and drinking water, Ehleringer et al. (2008) treated the fraction of non-exchangeable H in keratin that was fixed *in vivo*, f_s, as a fitting parameter. Likewise, the unconstrained or poorly constrained parameters α_{ow}, α_{hw}, and g were tuned to data consisting of paired hair-water samples. These parameters represent, respectively, (i) the isotope fractionation of carbonyl oxygen in hair relative to gut water, (ii) isotope fractionation of H in *de novo* synthesized amino acids relative to hair follicle water, and (iii) the fraction of O in the gut that derives from gastric juices rather than the water content of food.

Extension to O and H Isotopes of Hair in the Absence of Paired Water Samples: Bowen et al. (2009) later extended the modeling approach to mid-20th century indigenous populations. Unlike the prior work, this effort involved anthropological hair samples for which no corresponding drinking water data were recorded. This motivated two key modifications to the semi-mechanistic model and the corresponding introduction of three new parameters. Firstly, the authors posited a fraction of the diet ($0 < l < 1$) to be derived from local sources, as the populations in question lived a pre-globalization lifestyle and were geographically dispersed across several continents. Modeling food intake with stable isotopes identical to that supplied by a 21st century supermarket would be inappropriate in representing the dietary intake of these indigenous groups. Instead, a locally-derived component was assumed, and the relevant food isotopes were modeled as an offset ($\Delta(\delta^{18}O_l)$ and $\Delta(\delta^{2}H_l)$) from the average ^{2}H and ^{18}O content of regional precipitation. Use of these empirically determined offsets implicitly presumes a stable relationship between precipitation and the water used in agricultural endeavors (e.g. via ground water). Secondly, isotope signatures of regional precipitation were used as a measure of O and H isotopes in drinking water. With the model thus modified, parameters were adjusted to provide a good fit to data from several, geographically disparate indigenous groups.

The success of the Bowen et al. (2009) model in describing variations in O and H isotopes of hair as a function of drinking water (in this case, regional precipitation) is interesting in that it suggests that l, the fraction of diet derived from local sources, can be treated as a global constant. Hair samples from nearly all the indigenous groups fell along a common line indicating the same fraction of food being locally-derived. Furthermore, the non-local dietary contribution ($\delta^{18}O_d$, $\delta^{2}H_d$) was described using data representing supermarkets in the modern continental United States. Yet the hair samples represented populations in regions ranging from Canada to Pakistan to Botswana and a timespan between the 1930s and 1950s. Similarly, f_s, a physiological parameter likely to be subject to inter-individual variability, was treated as constant over all samples and individuals.

In this paper, we investigate the impact on model quality of using different approaches to represent the contributions of non-local and local diet to O and H isotopes of hair. Essentially, l is likely to differ based on socioeconomic, cultural, and biological differences between individuals, and that difference is critical to making quantitative links between hair and region of origin. Furthermore, we use statistical inference approaches to quantitatively assess the uncertainty inherent to these parameter estimates and consider their origin.

Materials and Methods

For this study, we used a subset of human hair samples (N = 62) from anonymous donors collected under NCSU IRB (#3285) and tap water samples (N = 76). Hair and water samples were collected by author CAJ, student assistants, and participating Catholic priests who were educated on the specifics of the IRB. For samples to be considered as part of this subset, at least two hair and water samples were required from the same location (city or town).

Sample Collection. All hair samples were obtained from anonymous confirmed residents from ten cities in six Mexican states (Table 1). Samples consisting of beard or scalp hair, representing several milligrams of material were collected on site in clean coin envelopes. City and state of residence, as well as date of collection, were recorded for each sample. Hair samples were collected between May and July and between December and January of 2014, 2015, 2017, and 2018. Unfiltered tap water samples were collected between December and January, May-July, and September- October in 2014, 2015, 2017, and 2018. All tap water samples were collected in acid washed 300ml, thick walled, HDPE bottles – following the recommendation of Spangenberg (2012) – with no head space (Spangenberg, 2012). Following collection, water and hair samples were stored in a temperature- and humidity-stable closet for a maximum period of two months. Samples were then sent to University of Utah SIRFER for analysis.

Hair Samples. Hair samples were solvent washed, weighed, and ground before being analyzed for ^{2}H and ^{18}O isotopes following the methods outlined in Thompson et al. (2010) and Bowen et al. (2005). Briefly, stable oxygen and hydrogen isotopic compositions in hair samples were calibrated relative to VSMOW scales using three laboratory reference standards (keratin: DS, ORX, and POW). Hair samples and the laboratory standards were equilibrated following Bowen et al. (2005) and stored under vacuum for a period of 5–7 days prior to analysis. The δ^{18}O and δ^2H values of encapsulated hair samples were measured on a ThermoFinnigan MAT 253 Isotope ratio mass spectrometer (IRMS) connected to a high temperature conversion elemental analyzer (TC/EA). All results for hydrogen data are expressed on a non-exchangeable hydrogen basis. The reference materials DS and ORX (assigned values δ^{18}O = 6.02 ‰ and 25.09 ‰, and δ^2H = –172.7 ‰ and –34.0 ‰ respectively) were used for calibration. Long term measurements of POW were used for quality control, (long term mean δ^{18}O =12.3 ‰, 1σ= ±0.1 ‰; δ^2H=100.5 ‰ 1σ= ±1.0 ‰ N=118). Laboratory reference materials consistently made up a minimum of 10% of the samples analyzed per run. Ten percent of hair samples were analyzed in duplicate. The measurement precision specific to the samples (the pooled standard deviation of all samples analyzed in duplicate) was ±0.6 ‰ for δ^2H and ±0.3 ‰ for δ^{18}O.

Water Samples. Tap water samples were calibrated relative to VSMOW scales using three laboratory reference standards (PZ, UT and PT). The δ^{18}O and δ^2H values of tap water were measured on a ThermoFinnigan MAT 253 Isotope ratio mass spectrometer (IRMS) connected to a high temperature conversion elemental analyzer (TC/EA). The reference materials PZ and UT (assigned values δ^{18}O = 1.65 ‰ and –16.5 ‰, and δ^2H = 16.9 ‰ and –123.1 ‰ respectively) were used for calibration. Long term measurements of PT (assigned value δ^{18}O = 7.25 ‰ and

δ^2H=46.0 ‰) were used for quality control, (long term mean $\delta^{18}O$ =7.1 ‰, 1σ= ±0.05 ‰; δ^2H=–45.8 ‰ 1σ= ±0.5 ‰ N=75). Laboratory reference materials consistently made up a minimum of 10% of the samples analyzed per run, and ten percent of water samples were analyzed in duplicate. The pooled standard deviation of all samples analyzed in duplicate was ±0.9 ‰ for δ^2H and ±0.5 ‰ for $\delta^{18}O$.

Hydrogen and oxygen isotopes from hair and water samples are expressed in per mil (‰) units relative to the international standard Vienna Standard Mean Ocean Water (VSMOW) using the standard delta notation $\delta X = 1000\ [R_{standard}/R_{sample} - 1]$. General statistical analysis was conducted in SPSS version 25. Parameter estimation for model fitting was performed in Matlab using the approach of approximate Bayesian computation.

Isotope Mapping Procedure. Analysis of spatial patterns of O and H isotopes in the tap water and hair data were conducted using ESRI's ArcGIS 10.3.1 and following the procedures specified in Bowen et al. (2007). Spatial patterning of isotope data was identified using the Spatial Autocorrelation tool (Spatial Statistics Toolbox, ArcGIS 10.3.1) which evaluates spatial autocorrelation using the Morans I statistic. Morans I statistics were calculated for δ^2H and $\delta^{18}O$ values using unstandardized weights derived from inverse-squared Euclidean distances between tap water sample data points. Isotope value prediction maps for δ^2H and $\delta^{18}O$ were produced through spatial interpolation of the raw tap water isotope survey data. Interpolation was accomplished through ordinary Kriging (Spatial Analyst Toolbox, ArcGIS 10.3.1) utilizing ArcGIS's Geostatistical Analyst extension. All kriging in this analysis was accomplished using a spherical semivariogram model.

Results and Analysis

Water Samples. Figure 2 shows the spatial variation of $\delta^{18}O$ and $\delta^{2}H$ isotopes in the samples (N=76) of Mexican tap water in the context of a larger tap water isoscape. The ten regions at the center of this study are indicated on the map. Isotope values of O and H of tap water in the 76 samples spanned a range from –11.4 ‰ to –4.3 ‰ and –79.1 ‰ to –22.5 ‰ for $\delta^{18}O$ and $\delta^{2}H$, respectively. Isotope levels in water samples differed in their standard deviation by collection location, ranging from 0.1 to 0.7 ‰ for $\delta^{18}O$ and 0.07 to 6.0 ‰ for $\delta^{2}H$. Samples from Oaxaca City showed the highest level of deviation. The calculated local meteoric water line (LMW) for tap waters was $\delta^{2}H = 8.6\ \delta^{18}O + 14.3$ ‰, $r^2 = 0.98$. The slope and d-excess parameter–a measure of proportions of ^{18}O and ^{2}H contained in water is a climatic indicator and a fingerprint of the oceanic source of precipitation– of the calculated LMW was slightly higher than the global meteoric water line ($\delta D=8.0\ \delta^{18}O +10$ ‰) calculated by Craig (1961). Wassenaar and colleagues (2009), previously reported two water lines for Mexico, the Mexican meteoric water line $\delta^{2}H = 7.5\ \delta^{18}O + 6.1$ ‰ defined by precipitation IAEA stations from three locations (Mexico City, Veracruz, and Chihuahua) and a ground water meteoric water line $\delta^{2}H = 7.9\ \delta^{18}O + 6.4$, $r^2 = 0.95$ based on their collected dataset (Wassenaar et al., 2009). Both the LMW generated from ground water and the combined Mexican LMW reported by Wassenar (2009) had lower slopes and d-excess parameters than either the GML or the tap water LMW, suggesting a bias toward slightly more negative values. For the groundwater values this may be explained by the focus on winter collection periods for ground water samples.

Hair Samples. Figure 3 shows the spatial variation of $\delta^{18}O$ and $\delta^{2}H$ isotopes in hair samples (N = 62) within the context of a larger tap water isoscape. For this sample, isotope content of hair ranged from +9.5 ‰ to +16.1 ‰ and –90.8 ‰ to –53.7 ‰ for $\delta^{18}O$ and $\delta^{2}H$, respectively. This range is slightly smaller than those previously reported by either Bowen et al. (2009), Ehleringer et al. (2008) or Thompson et al. (2010).

The most depleted $\delta^{18}O$ and $\delta^{2}H$ hair values came from individuals in the state of Morelos. As was the case for the water samples, standard deviation of isotope levels in hair differed by collection location. Standard deviations ranged from 0.2 ‰ to 1.1 ‰ and 1.0 ‰ and 8.7 ‰ for $\delta^{18}O$ and $\delta^{2}H$, respectively. Unlike in the case of the water samples, the moderate positive correlation between $\delta^{18}O$ and $\delta^{2}H$ in hair was not statistically significant ($r = 0.56$, $p = 0.087$). Indeed, an error-in-variables regression (which accounts for the standard deviation of isotope measurements) yields a relatively poor linear fit, as indicated by the 95% confidence bounds of the slope and intercept: $\delta^{2}H = 14.4\ [\pm 8.94]\ \delta^{18}O - 277\ [\pm 129]$ ‰. Cook's distance identified both the Veracruz groups as outliers. The Gutierrez Zamora population had a particularly irregular relationship between $\delta^{2}H$ isotopes in hair and water. The isotope values for water from Gutierrez Zamora were enriched relative to the rest of the sample subset. This makes sense given its coastal location. In contrast, the $\delta^{2}H$ isotopes in hair from Gutierrez Zamora were among the most depleted.

Empirical Relationships between Isotopes in Hair and Water for Paired Samples. The relationships between hair and water for this study and others are shown in Table 2. For our modern Mexican population, positive correlations between isotopes in hair and water were not significant, with correlation coefficients of $r = 0.61$ ($p = 0.05$) and $r = 0.60$ ($p = 0.06$) for ^{18}O and ^{2}H respectively. Error-in-variables regression yielded linear fits that were somewhat better for ^{2}H relative to ^{18}O: $\delta^{18}O_{h} = 0.183\ [\pm 0.132]\ \delta^{18}O_{tw} + 15.7\ [\pm 0.9]$ ‰ ($r^2 = 0.23$); $\delta^{2}H_{h} = 0.181$

[± 0.076] δ^2H_{tw} – 64.0 [± 3.0] ‰ (r^2 = 0.34). The corresponding coefficients of determination (r^2) indicate the extent to which variations in H and O in tap water explain isotope variations in hair. The lack of statistically significant correlations, large uncertainties in the linear regression parameters, and the low values of r^2 all point to tap water being a poor reference for predicting isotopes in hair for this population. This is in stark contrast to the prior work summarized in Table 2, where r^2 typically exceeds 70%.

In short, data from this Mexican population do not exhibit the strong relationships between isotopic values of tap water and hair that have been characteristic of other populations studied to date. This could be due to the prevalence of bottled water consumption in Mexico. Suppliers frequently draw their water from non-local aquifers and bodies of water. The problem is exaggerated in Mexico but, several authors have clearly demonstrated the complexities of drinking water distribution even in the familiar context of the United States (Jameel et al., 2013; Good et al., 2014; Tipple et al., 2017). Mismatches between water demand and availability can lead to municipal-level targeting of non-local water resources into other regions.

Modeling the Relationship between Isotopes in Hair and Water for Paired Samples. Given the economic stratification of this region and the poor correlation between hair and water samples, we chose to consider the possibility that l and f_s are local, rather than global, parameters for this population. Essentially, we assumed that both the fraction of diet that is locally-derived and the associated fraction of hydrogen that is fixed *in vivo* will differ across the sub-region depending on the relative affluence of the area, the particular sources of dietary protein, and the rural-urban divide. Taking that to be the case, we estimated a different value of l and f_s for each location. In line with the work of Ehleringer et al. (2008), we also estimated the water fractionation parameters α_{ow} and α_{hw}, treating them as global parameters common to all locations. For the ten-paired hair/water datasets reported in Table 1, we must then estimate more than 20 parameter values. With only one data point for each location, the model is severely under-determined, and a least-squares parameter estimation approach would not be appropriate. Instead, we infer plausible parameter intervals using the probabilistic approach of approximate Bayesian computation; this allows for the estimation of a likely distribution of values for each parameter, subject to a desire to minimize the difference between model predictions and the empirical data. From the resulting distributions, we determine an estimate for each parameter value and 95% bounds indicative of the uncertainty in that estimate. For example, the estimates obtained for α_{ow} α_{ow} and α_{hw} were 1.01 and 1.09 respectively, with 95% bounds of [1.00-1.03] and [1.07-1.10]. The α_{ow} estimate agrees with that reported by Ehleringer et al. (2008), $\alpha_{ow} = 1.016$, while our estimate for α_{hw} exceeds their tuned value of 1.002.

Characterizing the Isotope Content of Non-Local Dietary Sources: Given the anticipated importance of the non-local dietary contribution, we considered two different approaches to represent the isotopic signature of non-locally derived foods (i.e., δ^2H_d and $\delta^{18}O_d$). First, we employed the continental supermarket diet parameter values reported by Ehleringer et al. (2008) for the modern United States. We denote this model variant as “USA non-local”. Second, we treated the isotopic content of non-local food and the offset parameters (i.e. $\Delta(\delta^{18}O_l)$ and $\Delta(\delta^2H_l)$) for predicting isotopes in locally derived food as tuning parameters. We thereby proceeded to estimate the relevant values for this Mexican sub-region, denoting this model variant as “Mexico non-local”. O and H isotopes predicted on each of these bases were compared to the measurements made from paired hair samples.

Figures 4 A & B shows that using the USA non-local model generates a good fit for hydrogen data, but a relatively poor fit for oxygen data. Fit quality has been characterized via the isotope-specific contribution to the Bayesian computation summary statistic (ε), giving $\varepsilon_O = 7.0$ and $\varepsilon_H = 0.016$ for O and H, respectively. The orders-of-magnitude better fit for H data is due, in part, to fact that H values are tuneable using both f_s and l, whereas O values are only tuneable by l.

Figures 4 C & D demonstrate the impact of estimating both the local and non-local dietary contribution in the Mexico non-local model. In this case, O isotopic values are tuneable by adjustable parameters impacting both the non-local and the local diet contribution (specifically, non-local parameters $\delta^{18}O_d$, δ^2H_d and local offset parameters $\Delta(\delta^{18}O_l)$ and $\Delta(\delta^2H_l)$, which describe, respectively, the additive offsets of O and H isotopes in locally-derived foods from O and H isotopes in local water). Summary statistics demonstrate an improved fit for both O and H when local and non-local dietary parameters are estimated for the Mexican samples, *viz* $\varepsilon_O = 0.0053$ and $\varepsilon_H = 0.0018$. The estimated values for the Mexican non-local dietary signature and local diet offset were (mean [95% credibility interval]): δ^2H_d = –129 ‰ [–126, –132], $\delta^{18}O_d$ = +20.2 ‰ [19.5, 21.0], $\Delta(\delta^2H_l)$ = –35.8 ‰ [–32.8, –38.7] and $\Delta(\delta^{18}O_l)$ = +55.6 ‰ [52.8, 58.3]. The estimated non-local diet signatures are both depleted relative to those reported for the United States, *viz* δ^2H_d = –115 ‰, $\delta^{18}O_d$ = +26 ‰ (Ehleringer et al. 2008). The local diet offsets are instead enriched relative to the USA estimates of $\Delta(\delta^2H_l)$ = –50 ‰ and $\Delta(\delta^{18}O_l)$ = +35.4 ‰ (Bowen et al. 2009).

Contextualizing *l* and *f*s with Respect to the Rural-Urban Divide and Socioeconomic Stratification: Figure 5 shows the estimates for l and f_s obtained with each model variant. Estimations of l using the "USA non-local" approach (Figure 5A & C) are shown above those obtained using the “Mexico non-local” approach (Figure 5B & D). Data are displayed as histograms representing the credible intervals of parameter estimates. Values for *l* demonstrate significant shifts between the USA non-local and Mexico non-local framings. For example, local dietary contributions (*l*) for Mexico City, Tultepec (Mexico State), Oaxaca City, Cuernavaca, Palenque, and Papantla were reduced considerably. For f_s, the Mexican estimates are suggestive of much lower quality protein consumption (i.e., they increase f_s) for all locations except Tultepec (Mexico State), Cuernavaca, and Gutiérrez Zamora.

The USA non-local model produces estimates of local dietary contributions that appear inconsistent with what might be expected based on SES. For example, individuals living in major urban centers like Mexico City and Cuernavaca and in rural parts of Michoacán (Patzcuaro and Tzintzuntzan) are estimated to have virtually indistinguishable local food contributions. In the absence of additional data on food or orthogonal isotope data for hair (e.g., carbon, nitrogen), we cannot confirm the validity of the estimated value of *l* for each region. However, we can look at distinctions between large urban centers and more rural areas. Use of the Mexico non-local model repositions urban centers like Mexico City, Oaxaca City, and Cuernavaca toward lower values for *l* and more rural centers like Tzintzuntzan and Patzcuaro shift to higher values for *l*. One interpretation of this is that urban residents have increased access to non-local foods versus their more rural counterparts. The position of Palenque and Mexico state as the two locations with the lowest estimated values for *l* is interesting, as data on socioeconomic status in Mexico identifies these two states as polar economic opposites (Figure 6).

One interpretation of f_s is as an indicator of protein consumption, with lower values of f_s associated with increased protein consumption. The USA non-local model appears to overestimate protein consumption across all locations, while use of the Mexico-specific parameters may underestimate protein consumption for the dataset. Studies on obesity and health in Mexico indicate that the majority of calories in the daily diet of Mexicans comes from carbohydrates (>60%) while proteins make up only ~11% of caloric intake (Heien et al., 1989; Fernald et al., 2004; Ruiz-Arregui et al., 2007; Ortiz-Hernández and Gómez-Tello, 2008; Sparks and Sparks, 2012). In principle, this supports the values for f_s estimated in the Mexico non-local model. Coastal locations like Gutierrez Zamora, where marine protein likely contributes a unique isotopic signature to the local diet would be expected to yield spurious predictions in this modeling framework. This is evident in the l and f_s predictions for the Mexico non-local model, where a reasonable value of l (~60%) is coupled with an inappropriately low value of f_s (<0.05).

In the absence of carbon and nitrogen isotopes in food and hair for the region, we cannot ascertain the relative validity of the l and f_s estimates. However, if we assume that these parameters reflect something about SES of the populations in questions, we can attempt to interpret the parameter estimates in the context of marginality indices (MI). The marginality index is a summary measure, expressed on a scale of 0 to 100, that differentiates states and municipalities according to the overall impact of deficiencies such as lack of access to education, residence in inadequate housing, insufficient monetary income, and rural living. The Consejo Nacional de Población (CONAPO, the Mexican national council on population) uses census data to generate marginality indices every ten years (Vertiz, 2011). Although MI tells us nothing about the circumstances of any individual in a particular region, it serves as a coarse characterization of population-level SES differences. Figure 6 shows the MI map for our region of interest, with the hair and water sampling locations indicated. Comparing marginality to either l or f_s, we see no consistent pattern in the predictions for either model variant. In the USA non-local model, the low MI cities of Cuernavaca, Mexico City, Patzcuaro, and Tultepec do appear with similar l ($l > 0.45$). However, the high MI, relatively impoverished town of Palenque appears with l in the same range. Similarly, these locations do not segregate with respect to MI when we consider the USA non-local model estimates for f_s. The same is true in the case of the Mexico non-local model; in the l and f_s predictions, no consistent pattern is observed with respect to MI. Where this model variant does succeed is in segregating rural and urban locations with respect to l. We posit that this reflects situational differences in access to non-local foods.

Discussion

We quantified the relationship between modern Mexican hair and water samples using a modified approach to the semi-mechanistic framework established by Bowen et al. (2009). By linear regression, we found that, although O and H isotopes in water and hair maintain similar geographic distributions, O and H isotopes in tap water explain only a small part of the variation observed in hair samples. Thus, the Mexican data do not represent a consistent trend between hair and tap water, but rather a more nuanced connection between nominally available drinking water and O and H isotopes of hair. Rather than a straightforward one-to-one mapping of hair to water, multiple factors alter the relative importance of water and dietary contributions. Quantification of multiple isotopes and the estimation of additional parameters was needed to tease out the underlying details. Indeed, a visually-compelling fit to the paired H data was possible whether USA established values or Mexican estimates were used for the non-local dietary contributions. However, the failure to match paired O data and the counterintuitive values estimated for local diet fraction, l, argue against the USA non-local diet basis for the model. Instead, the Mexican estimates for non-local diet and local diet offsets, which are consistently depleted of ^{18}O and ^{2}H relative to the USA supermarket diet, permit regional distributions of l

and f_s that cleanly segregate affluent urban areas like Mexico City from rural towns like Quiroga. Likewise, the coastal city of Gutierrez Zamora is clearly distinguished, probably because of a high-protein, seafood-based diet conferring a low f_s parameter.

In principle, this lack of a strong correlation between sole-source water and hair is in line with the complex relationships that modern Mexicans have with drinking water. In many areas in Mexico, tap water is safe to drink and is used for drinking, cooking, and bathing. In other locations, bottled water, precipitation or a combination of both is the source for all water needs. These disparate water-use practices may occur in the same state for cities within close geographical proximity. Disparities will also exist for individuals in the same city who have very different economic status. With SES impacting both food and water access, it is likely that increasingly complex models and analytical approaches that quantify variability and uncertainty will be needed to support provenience estimation. In this case, our understanding and interpretation of the data was assisted by firsthand observation of the populations in this region over several years. This includes observation of migration behaviors. For forensic scientists interested in using H and O isotopes in hair and water for provenance analysis on Mexican populations, cultural competency is critical to developing successful modeling approaches.

Acknowledgements

The Authors would like to acknowledge Abril Camarillo, Benny Sandoval, and Padre Juan Be for assistance with sample collection.

Received 1 November 2018; accepted for publication 9 March 2019.

Literature Cited

Arcega-Cabrera, F., L. F. Fargher, I. Oceguera-Vargas et al. 2017. Water consumption as source of arsenic, chromium, and mercury in children living in rural Yucatan, Mexico: Blood and urine levels. *Bull. Environ. Contam. Toxicol*. 99:452–459.

Armienta, M. A., and N. Segovia. 2008. Arsenic and fluoride in the groundwater of Mexico. *Environ. Geochem. Health* 30:345–353.

Ayala, A. G., and M. J. O'Rourke. 1989. Effects of the 1985 Michoacán earthquake on water systems and other buried lifelines in Mexico. Techical Report NCEER-89-0009. Buffalo, NY: National Center for Earthquake Engineering Research.

Bataille, C. P., and G. J. Bowen. 2012. Mapping $^{87}Sr/^{86}Sr$ variations in bedrock and water for large scale provenance studies. *Chem. Geol*. 304–305:39–52.

Borroto, R. J., and R. Martinez-Piedra. 2000. Geographical patterns of cholera in Mexico, 1991–1996. *Int. J. Epidemiol*. 29:764–772.

Bowen, G. J., J. R. Ehleringer, L. A. Chesson et al. 2007. Stable isotope ratios of tap water in the contiguous United States. *Water Resour. Res*. 43:1–12.

Bowen, G. J., J. R. Ehleringer, L. A. Chesson et al. 2009. Dietary and physiological controls on the hydrogen and oxygen isotope ratios of hair from mid-20th century indigenous populations. *Am. J. Phys. Anthropol*. 139:494–504.

Bowen, G. J., D. A. Winter, H. J. Spero et al. 2005. Stable hydrogen and oxygen isotope ratios of bottled waters of the world. *Rapid Commun. Mass Spectrom*. 19:3,442–3,450.

Bundschuh, J., M. I. Litter, F. Parvez et al. 2012. One century of arsenic exposure in Latin America: A review of history and occurrence from 14 countries. *Sci. Total Environ*. 429:2–35.

Chesson, L. A., J. E. Barnette, G. J. Bowen et al. 2018. Applying the principles of isotope analysis in plant and animal ecology to forensic science in the Americas. *Oecologia* 187:1,077–1,094.

Chesson, L. A., D. W. Podlesak, B. R. Erkkila et al. 2010. Isotopic consequences of consumer food choice: Hydrogen and oxygen stable isotope ratios in foods from fast food restaurants versus supermarkets. *Food Chem*. 119:1,250–1,256.

Davis, D. E. 2005. Reverberations: Mexico City's 1985 earthquake and the transformation of the capital. In *The Resilient City: How Modern Cities Recover from Disaster*, L. J. Vale and T. J. Campanella, eds. Oxford: Oxford University Press, 255–280.

Ehleringer, J. R., G. J. Bowen, L. A. Chesson et al. 2008. Hydrogen and oxygen isotope ratios in human hair are related to geography. *Proc. Natl. Acad. Sci. U. S. A.* 105:2,788–2,793.

Ehleringer, J. R., A. H. Thompson, D. W. Podlesak et al. 2010. A framework for the incorporation of isotopes and isoscapes in geospatial forensic investigations. In *Isoscapes: Understanding Movement, Pattern, and Process on Earth through Isotope Mapping*, J. B. West, T. E. Dawson, G. J. Bowen, and K. P. Tu, eds. New York: Springer, 357–387.

Espinosa-García, A. C., C. Díaz-Ávalos, F. J. González-Villarreal et al. 2015. Drinking water quality in a Mexico City university community: Perception and preferences. *Ecohealth* 12:88–97.

Fernald, L. C., J. P. Gutierrez, L. M. Neufeld et al. 2004. High prevalence of obesity among the poor in Mexico. *JAMA* 291:2,544–2,545.

Franco, J., L. Mehta, and G. J. Veldwisch. 2015. The global politics of water grabbing. In *Global Land Grabs: History, Theory and Method*, M. Edleman, C. Oya, and S. M. Borras Jr., eds. London: Routledge, 135–159.

Good, S. P., C. D. Kennedy, J. C. Stalker et al. 2014. Patterns of local and nonlocal water resource use across the western U.S. determined via stable isotope intercomparisons. *Water Resour. Res*. 50:8,034–8,049.

Greene, J. C. 2014. The bottled water industry in Mexico. Master's thesis, University of Texas Austin.

Gutieŕrez, R., S. Vega, R. Ortiz et al. 2012. Presence of organochlorine contaminants in bottled drinking water from Mexico City. *Water Sci. Technol. Water Supply* 12:470–479.

Heien, D., L. S. Jarvis, and F. Perali. 1989. Food consumption in Mexico: Demographic and economic effects. *Food Policy* 14:167–179.

Hernandez-Cortazar, I. B., K. Y. Acosta-Viana, E. Guzman-Marin et al. 2017. Presence of *Toxoplasma gondii* in drinking water from an endemic region in southern Mexico. *Foodborne Pathog. Dis*. 14:288–292.

Hobson, K. A., L. Atwell, and L. I. Wassenaar. 1999. Influence of drinking water and diet on the stable-hydrogen isotope ratios of animal tissues. *Proc. Natl. Acad. Sci. U. S. A.* 96:8,003–8,006.

Jameel, Y., S. Brewer, S. P. Good et al. 2016. Tap water isotope ratios reflect urban water system structure and dynamics across a semiarid metropolitan area. *Water Resour. Res*. 52:5,891–5,910.

Meier-Augenstein, W., and I. Fraser. 2008. Forensic isotope analysis leads to identification of a mutilated murder victim. *Sci. Justice* 48:153–159.

Meier-Augenstein, W., and H. F Kemp. 2010. Human provenancing based on stable isotope forensic intelligence. *Sci. Justice* 50:35–36.

Montero-Contreras, D. P. 2016. El consumo de agua embotellada en la Ciudad de México desde una perspectiva institucional. *Agua y Territorio* 7:35–49

O'Brien, D. M., and M. J. Wooller. 2007. Tracking human travel using stable oxygen and hydrogen isotope analyses of hair and urine. *Rapid Commun. Mass Spectrom*. 21:2,422–2,430.

Ortiz-Hernández, L., and B. L. Gómez-Tello. 2008. Food consumption in Mexican adolescents. *Rev. Panam. Salud. Publica*. 24:127–135.

Pani, M. 2017. Accelerating Towards Excellence: Coca-Cola FEMSA Sustainability Report 2016. Mexico City.

Podlesak, D. W., G. J. Bowen, S. O'Grady et al. 2012. δ^2H and δ^{18}O of human body water: A GIS model to distinguish residents from non-residents in the contiguous USA. *Isotopes Environ. Health Stud*. 48:259–279.

Podlesak, D. W., A. M. Torregrossa, J. R. Ehleringer et al. 2008. Turnover of oxygen and hydrogen isotopes in the body water, CO_2, hair, and enamel of a small mammal. *Geochim. Cosmochim. Acta* 72:19–35.

Rodríguez-Tapia, L., D. Revollo-Fernández, and J. Morales-Novelo. 2017. Household's perception of water quality and willingness to pay for clean water in Mexico City. *Economies* 5:12.

Ross, A. H., C. A. Juarez, and P. Urbanová. 2016. Complexity of assessing migrant death place of origin. In *Biological Distance Analysis: Forensic and Bioarchaeological Perspectives*, M. A. Pilloud and J. T. Hefner, eds. London: Elsevier, 265–283.

Ruiz-Arregui, L., L. Castillo-Martínez, A. Orea-Tejeda et al. 2007. Prevalence of self-reported overweight-obesity and its association with socioeconomic and health factors among older Mexican adults. *Salud Publica Mex.* 49, Suppl 4:S482-S487.

Russell, A. L., and E. Elvove. 1962. Domestic water and dental caries. VII. A study of the fluoride-dental caries relationship in an adult population. In *Fluoride Drinking Waters: A Selection of Public Health Service Papers on Dental Fluorosis and Dental Caries; Physiological Effects, Analysis and Chemistry of Fluoride,* F. J. McClure, ed. Bethesda, MD: U.S. Department of Health, Education, and Welfare, 166–172.

Sepúlveda, J., J. L. Valdespino, and L. García-García. 2006. Cholera in Mexico: The paradoxical benefits of the last pandemic. *Int. J. Infect. Dis*. 10:4–13.

Sharp, Z. D., V. Atudorei, H. O. Panarello et al. 2003. Hydrogen isotope systematics of hair: Archeological and forensic applications. *J. Archaeol. Sci*. 30:1,709–1,716.

Sosa-Rodriguez, F. S. 2012. Assessing water quality in the developing world : An index for Mexico City. In *Water Quality Monitoring and Assessment,* K. Voudouris, ed. London: InTech, 495–508. Retrieved from: https://www.intechopen.com/books/water-quality-monitoring-and-assessment/assessing-water-quality-in-the-developing-world-an-index-for-mexico-city.

Spangenberg, J. E. 2012. Caution on the storage of waters and aqueous solutions in plastic containers for hydrogen and oxygen stable isotope analysis. *Rapid Commun. Mass Spectrom*. 26:2,627–2,636.

Sparks, P. J., and C. S. Sparks. 2012. Socioeconomic position, rural residence, and marginality influences on obesity status in the adult Mexican population. *Int. J. Popul. Res*. 2012:1–13.

Spring, Ú. O. 2014. Water security and national water law in Mexico. *Earth Perspectives* 1:7.

Thompson, A. H., L. A. Chesson, D. W. Podlesak et al. 2010. Stable isotope analysis of modern human hair collected from Asia (China, India, Mongolia, and Pakistan). *Am. J. Phys. Anthropol*. 141:440–451.

Tipple, B. J., Y. Jameel, T. H. Chau et al. 2017. Stable hydrogen and oxygen isotopes of tap water reveal structure of the San Francisco Bay Area's water system and adjustments during a major drought. *Water Res*. 119:212–224.

Vertiz, J. M. 2011. Índice de Marginación por Entidad Federativa y Municipio 2010. Mexico City. http://www.conapo.gob.mx/en/CONAPO/Indices_de_Marginacion_2010_por_entidad_federativa_y_municipio.

Warner, M. M., A. M. Plemons, N. P. Herrmann et al. 2018. Refining stable oxygen and hydrogen isoscapes for the identification of human remains in Mississippi. *J. Forensic Sci*. 63:395–402.

Wassenaar, L. I., S. L. Van Wilgenburg, K. Larson et al. 2009. A groundwater isoscape (δD, δ^{18}O) for Mexico. *J. Geochem. Explor*. 102:123–136.

West, J. B., H. W. Kreuzer, and J. R. Ehleringer. 2010. Approaches to plant Hydrogen and Oxygen Isoscapes Generation. In *Isoscapes: Understanding Movement, Pattern, and Process on Earth through Isotope Mapping*, J. B. West, T. E. Dawson, G. J. Bowen, and K. P. Tu, eds. New York: Springer, 161–178.

Williams, L. J., C. D. White, and F. J. Longstaffe. 2011. Improving stable isotopic interpretations made from human hair through reduction of growth cycle error. *Am. J. Phys. Anthropol*. 145:125–136.

Wolfe, M. D. 2017. *Watering the Revolution: An Environmental and Technological History of Agrarian Reform in Mexico*. Durham, NC: Duke University Press.

World Health Organization (WHO) and United Nations Children's Fund (UNICEF). 2017. *Progress on Drinking Water, Sanitation and Hygiene: 2017 Update and SDG Baselines.* License: CC BY-NC-SA 3.0 IGO.

Table 1. Summary of Hair and Tap Water Isotope Ratios by City

State	City		$\delta^{18}O_h$	δ^2H_h	$\delta^{18}O_{tw}$	δ^2H_{tw}
Mexico	Mexico City	mean	+12.3 ‰	–76.9 ‰	–9.5 ‰	–68 ‰
		SD	±1.1 ‰	±4.7 ‰	±0.6 ‰	±3.9 ‰
		N	10	10	15	15
Mexico	Tultepec	mean	+11.7 ‰	–83.3 ‰	–9.3 ‰	–66.6 ‰
		SD	±1.0 ‰	±5.7 ‰	±0.3 ‰	±2.2 ‰
		N	5	5	5	5
Oaxaca	Oaxaca City	mean	+12.5 ‰	–75.2 ‰	–9.4 ‰	–68.3 ‰
		SD	±0.9 ‰	±8.7 ‰	±0.7 ‰	±6.6 ‰
		N	15	15	22	22
Michoacán	Tzintzuntzan	mean	+14.5 ‰	–74.5 ‰	–10.0 ‰	–73.4 ‰
		SD	±0.3 ‰	±3.1 ‰	±0.2 ‰	±0.8 ‰
		N	5	5	5	5
Michoacán	Pátzcuaro	mean	+14.8 ‰	–69.2 ‰	–9.3 ‰	–67.3 ‰
		SD	±1.1 ‰	±2.3 ‰	±0.1 ‰	±0.1 ‰
		N	5	5	4	4
Michoacán	Quiroga	mean	+14.5 ‰	–78.4 ‰	–9.3 ‰	–67.5 ‰
		SD	±1.0 ‰	±2.0 ‰	±0.1 ‰	±0.9 ‰
		N	5	5	4	4
Morelos	Cuernavaca	mean	+12.5 ‰	–78.4 ‰	–11.1 ‰	–77.4 ‰
		SD	±0.7 ‰	±7.2 ‰	±0.3 ‰	±2.1‰
		N	5	5	8	8
Chiapas	Palenque	mean	+14.5 ‰	–66.1 ‰	–4.6 ‰	–24.5 ‰
		SD	±0.2 ‰	±1.0 ‰	±0.3 ‰	±1.5 ‰
		N	4	4	4	4
Veracruz	Papantla	mean	+15.1 ‰	–56.0 ‰	–5.0 ‰	–27.7 ‰
		SD	±0.4 ‰	±2.3 ‰	±3.8 ‰	±0.5 ‰
		N	4	4	4	4
Veracruz	Gutierrez Zamora	mean	+15.4 ‰	–78.3 ‰	–5.0 ‰	–26.5 ‰
		SD	±0.5 ‰	±1.3 ‰	±0.3 ‰	±1.5 ‰
		N	4	4	5	5

h = hair; tw = tap water

Table 2. Published Regression Relationships for Hair and Water

Study	Population / Region	Water type	Hair N	$\delta^2H_w = m\ \delta^{18}O_w + b$	$\delta^2H_h = m\ \delta^{18}O_h + b$	$\delta^{18}O_h = m\ \delta^{18}O_w + b$	$\delta^2H_h = m\ \delta^2H_w + b$
Bowen et al. (2009)	Museum Collection (1935-66)/ Global*	precip	123		$\delta^2H_h = 8.86\ \delta^{18}O_h - 203$ ‰ $r^2 = 0.75$; $p < 0.001$	$\delta^{18}O_h = 0.70\ \delta^{18}O_w + 10.2$ ‰ $r^2 = 0.77$; $p < 0.001$	$\delta^2H_h = 0.78\ \delta^2H_w - 49.5$ ‰ $r^2 = 0.90$; $p < 0.001$
Thompson et al. (2010)	Modern / China India Mongolia Pakistan	tap water	196	$\delta^2H_w = 6.9\ \delta^{18}O_w - 5.5$ ‰ $r^2 = 0.97$	$\delta^2H_h = 5.64\ \delta^{18}O_h - 172$ ‰ $r^2 = 0.80$, $p < 0.01$	$\delta^{18}O_h = 0.40\ \delta^{18}O_w + 16.4$ ‰ $r^2 = 0.79$; $p < 0.001$	$\delta^2H_h = 0.42\ \delta^2H_w - 75$ ‰ $r^2 = 0.75$; $p < 0.001$
Ehleringer et al. (2008)	Modern/ USA	tap water	65	$\delta^2H_w = 7.87\ \delta^{18}O_w + 4.4$ ‰ $r^2 = 0.98$; $p < 0.001$	$\delta^2H_h = 5.73\ \delta^{18}O_h - 166$‰ $r^2 = 0.873$; $p < 0.001$	$\delta^{18}O_h = 0.35\ \delta^{18}O_w + 15.2$ ‰ $r^2 = 0.86$; $p < 0.001$	$\delta^2H_h = 0.27\ \delta^2H_w - 79$ ‰ $r^2 = 0.86$; $p < 0.001$
O'brien and Wooller (2007)	Modern/ USA		10		$\delta^2H_h = 8.53\ \delta^{18}O_h - 182.7$ ‰ $r^2 = 0.70$; $p = 0.004$		
This study	Modern/ Mexico	tap water	62	$\delta^2H_w = 8.6\ \delta^{18}O_w + 14.3$ ‰ $r^2 = 0.98$; $p < 0.001$	$r = 0.56$; $p = 0.089$	$r = 0.61$; $p = 0.05$	$r = 0.60$; $p = 0.06$

*Thailand, Japan, Canada, Pakistan, USA, Venezuela, Australia, South Africa, Botswana, Guatemala, Mexico, Zambia

Supplementary Table S1. Hair and Tap Water δ^{18}O and δ^{2}H Isotope Ratios by City (Individual Samples)

State	City	$\delta^{18}O_h$ ‰	$\delta^{2}H_h$ ‰	$\delta^{18}O_{tw}$ ‰	$\delta^{2}H_{tw}$ ‰
Mexico	Mexico City	+12.7 ‰	–83.4 ‰	–9.7 ‰	–70.3 ‰
Mexico	Mexico City	+12.1 ‰	–75.2 ‰	–8.5 ‰	–62.4 ‰
Mexico	Mexico City	+12.5 ‰	–75.2 ‰	–8.8 ‰	–63.6 ‰
Mexico	Mexico City	+11.6 ‰	–84.5 ‰	–10.0 ‰	–70.7 ‰
Mexico	Mexico City	+13.2 ‰	–75.3‰	–10.2 ‰	–72.1 ‰
Mexico	Mexico City	+9.5 ‰	–71.0 ‰	–10.5 ‰	–73.1 ‰
Mexico	Mexico City	+12.8 ‰	–75.1 ‰	–9.7 ‰	–71.0 ‰
Mexico	Mexico City	+13.5 ‰	–73.0 ‰	–9.0 ‰	–68.3 ‰
Mexico	Mexico City	+12.1 ‰	–82.4 ‰	–9.3 ‰	–65.7 ‰
Mexico	Mexico City	+12.3 ‰	–74.2 ‰	–9.5 ‰	–67.6 ‰
Mexico	Mexico City			–9.0 ‰	–69.6 ‰
Mexico	Mexico City			–9.0 ‰	–62.0 ‰
Mexico	Mexico City			–10.1 ‰	–71.8 ‰
Mexico	Mexico City			–8.8 ‰	–71.0 ‰
Mexico	Mexico City			–9.9 ‰	–70.0 ‰
Mexico	Tultepec	+11.1 ‰	–90.0 ‰	–9.3 ‰	–65.7 ‰
Mexico	Tultepec	+13.5 ‰	–74.7 ‰	–9.5 ‰	–67.6 ‰
Mexico	Tultepec	+11.7 ‰	–81.9 ‰	–9.1 ‰	–64.2 ‰
Mexico	Tultepec	+10.7 ‰	–86.5 ‰	–9.0 ‰	–65.8 ‰
Mexico	Tultepec	+12.0 ‰	–83.0 ‰	–9.9 ‰	–69.9 ‰
Oaxaca	Oaxaca City	+12.3 ‰	–67.5 ‰	–8.8 ‰	–62.1‰
Oaxaca	Oaxaca City	+11.0 ‰	–89.8 ‰	–10.2 ‰	–76.1 ‰
Oaxaca	Oaxaca City	+14.3 ‰	–71.2 ‰	–9.4 ‰	–70.4 ‰
Oaxaca	Oaxaca City	+13.0 ‰	–73.9 ‰	–9.3 ‰	–67.5 ‰
Oaxaca	Oaxaca City	+11.6 ‰	–69.5 ‰	–8.5 ‰	–62.7 ‰
Oaxaca	Oaxaca City	+11.5 ‰	–71.8 ‰	–8.2 ‰	–59.5 ‰
Oaxaca	Oaxaca City	+13.7 ‰	–74.8 ‰	–10.2 ‰	–75.9 ‰
Oaxaca	Oaxaca City	+13.7 ‰	–68.9 ‰	–8.9 ‰	–62.6 ‰
Oaxaca	Oaxaca City	+12.0 ‰	–59.7 ‰	–10.5 ‰	–77.8 ‰
Oaxaca	Oaxaca City	+12.8 ‰	–77.6 ‰	–9.7 ‰	–71.3 ‰
Oaxaca	Oaxaca City	+12.1‰	–84.5 ‰	–7.6 ‰	–52.9 ‰
Oaxaca	Oaxaca City	+12.9 ‰	–70.9 ‰	–9.1 ‰	–66.0 ‰
Oaxaca	Oaxaca City	+11.9 ‰	–90.8 ‰	–8.8 ‰	–60.5 ‰
Oaxaca	Oaxaca City	+12.4 ‰	–73.8 ‰	–9.3 ‰	–68.6 ‰

Oaxaca	Oaxaca City	+11.8 ‰	–84.8 ‰	–9.4 ‰	–65.9 ‰
Oaxaca	Oaxaca City			–8.9 ‰	–62.2 ‰
Oaxaca	Oaxaca City			–9.7 ‰	–72.2 ‰
Oaxaca	Oaxaca City			–10.5 ‰	–74.9 ‰
Oaxaca	Oaxaca City			–9.4 ‰	–66.9 ‰
Oaxaca	Oaxaca City			–10.0 ‰	–71.2 ‰
Oaxaca	Oaxaca City			–9.8 ‰	–69.3 ‰
Oaxaca	Oaxaca City			–9.7 ‰	–75.7 ‰
Michoacán	Tzintzuntzan	+14.3 ‰	–75.9 ‰	–10.1 ‰	–73.7 ‰
Michoacán	Tzintzuntzan	+15.0 ‰	–71.1 ‰	–10.0 ‰	–73.2 ‰
Michoacán	Tzintzuntzan	+14.4 ‰	–77.3 ‰	–9.7 ‰	–72.0 ‰
Michoacán	Tzintzuntzan	+14.1 ‰	–77.2 ‰	–10.0 ‰	–74.0 ‰
Michoacán	Tzintzuntzan	+14.7 ‰	–71.2 ‰	–10.1 ‰	–73.8 ‰
Michoacán	Pátzcuaro	+14.6 ‰	–69.2 ‰	–9.5 ‰	–67.4 ‰
Michoacán	Pátzcuaro	+15.9 ‰	–70.8 ‰	–9.3 ‰	–67.3 ‰
Michoacán	Pátzcuaro	+14.1 ‰	–67.1 ‰	–9.3 ‰	–67.3 ‰
Michoacán	Pátzcuaro	+13.3 ‰	–71.2 ‰	–9.2 ‰	–67.2 ‰
Michoacán	Quiroga	+14.5 ‰	–78.4 ‰	–9.3 ‰	–67.5 ‰
Michoacán	Quiroga	+13.1 ‰	–77.1 ‰	–9.4 ‰	–66.2 ‰
Michoacán	Quiroga	+14.9 ‰	–79.0 ‰	–9.4 ‰	–68.0 ‰
Michoacán	Quiroga	+14.2 ‰	–76.2 ‰	–9.1 ‰	–68.2 ‰
Michoacán	Quiroga	+15.8 ‰	–81.3 ‰		
Morelos	Cuernavaca	+12.8 ‰	–73.1 ‰	–11.2 ‰	–78.9 ‰
Morelos	Cuernavaca	+13.0 ‰	–77.2 ‰	–11.3 ‰	–78.1 ‰
Morelos	Cuernavaca	+11.4 ‰	–90.8 ‰	–11.5 ‰	–79.2 ‰
Morelos	Cuernavaca	+13.0 ‰	–74.0 ‰	–11.0 ‰	–77.6 ‰
Morelos	Cuernavaca	+12.6 ‰	–76.7 ‰	–10.4 ‰	–72.5 ‰
Morelos	Cuernavaca			–11.3 ‰	–78.1 ‰
Morelos	Cuernavaca			–11.0 ‰	–76.5 ‰
Morelos	Cuernavaca			–11.1‰	–78.0 ‰
Chiapas	Palenque	+14.2 ‰	14.2 ‰	–4.9 ‰	–25.5 ‰
Chiapas	Palenque	+14.5 ‰	14.5 ‰	–4.4 ‰	–23.6 ‰
Chiapas	Palenque	+14.6 ‰	14.6 ‰	–4.8 ‰	–22.9 ‰
Chiapas	Palenque	+14.7 ‰	14.7 ‰	–4.3 ‰	–25.9 ‰
Veracruz	Papantla	+14.7 ‰	–57.7 ‰	–5.5 ‰	–31.4 ‰
Veracruz	Papantla	+15.5 ‰	–54.4 ‰	–4.3 ‰	–25.8 ‰
Veracruz	Papantla	+14.9 ‰	–53.7 ‰	–4.8 ‰	–22.5 ‰
Veracruz	Papantla	+15.6 ‰	–58.4 ‰	–5.1 ‰	–27.0 ‰

Veracruz	Gutiérrez Zamora	+15.4 ‰	–78.3 ‰	–5.1 ‰	–28.5 ‰
Veracruz	Gutiérrez Zamora	+15.1 ‰	–79.9 ‰	–5.0 ‰	–25.7 ‰
Veracruz	Gutiérrez Zamora	+14.9 ‰	–78.3 ‰	–4.8 ‰	–25.3 ‰
Veracruz	Gutiérrez Zamora	+16.1 ‰	–76.6 ‰	–4.3 ‰	–25.5 ‰
Veracruz	Gutiérrez Zamora			–5.1 ‰	–27.6 ‰

h = hair; tw = tap water; blank space mean no sample.

Figure 1.

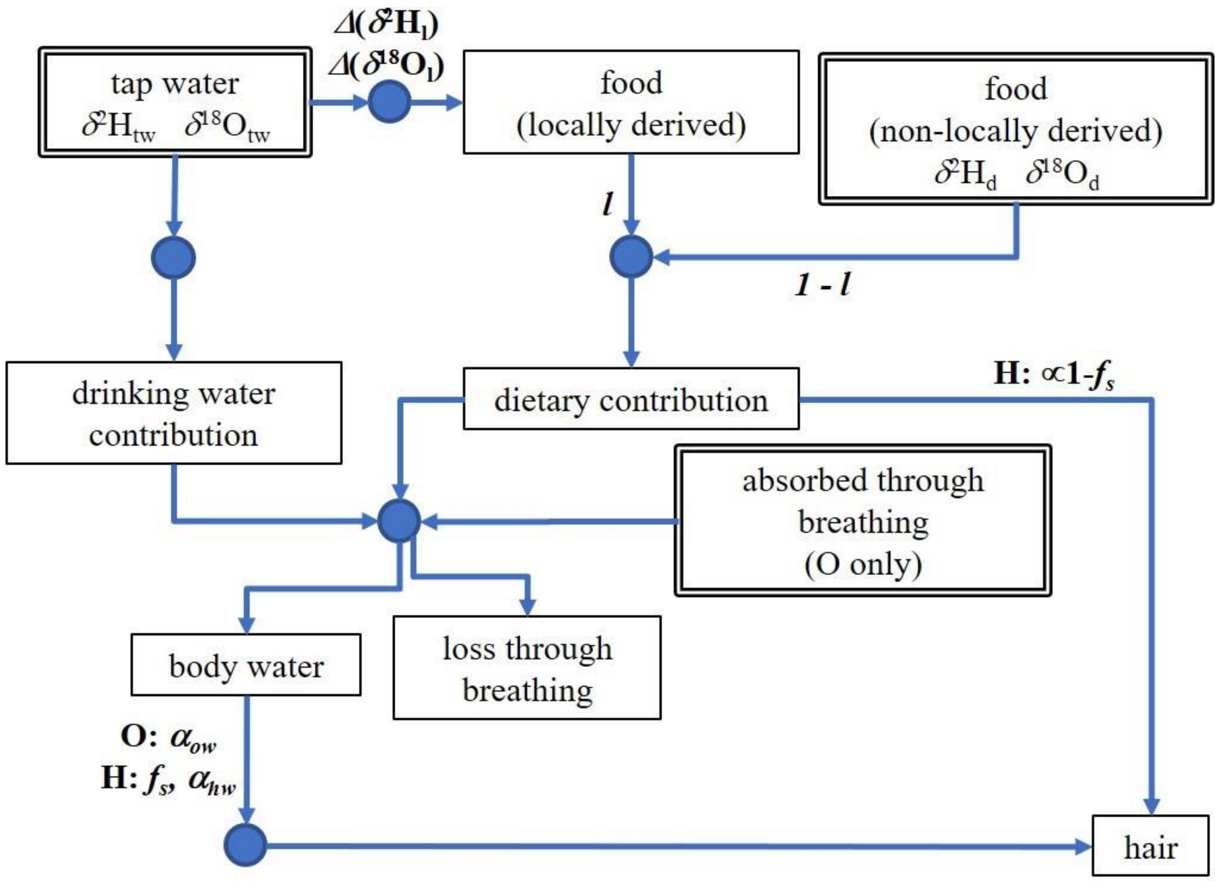

tap water
δ^2H_{tw} $\delta^{18}O_{tw}$
$\Delta(\delta^2H_l)$
$\Delta(\delta^{18}O_l)$
food
(locally derived)
food
(non-locally derived)
δ^2H_d $\delta^{18}O_d$
l
$1 - l$
drinking water contribution
dietary contribution
H: $\propto 1-f_s$
absorbed through breathing
(O only)
body water
loss through breathing
O: α_{ow}
H: f_s, α_{hw}
hair

Figure 2.

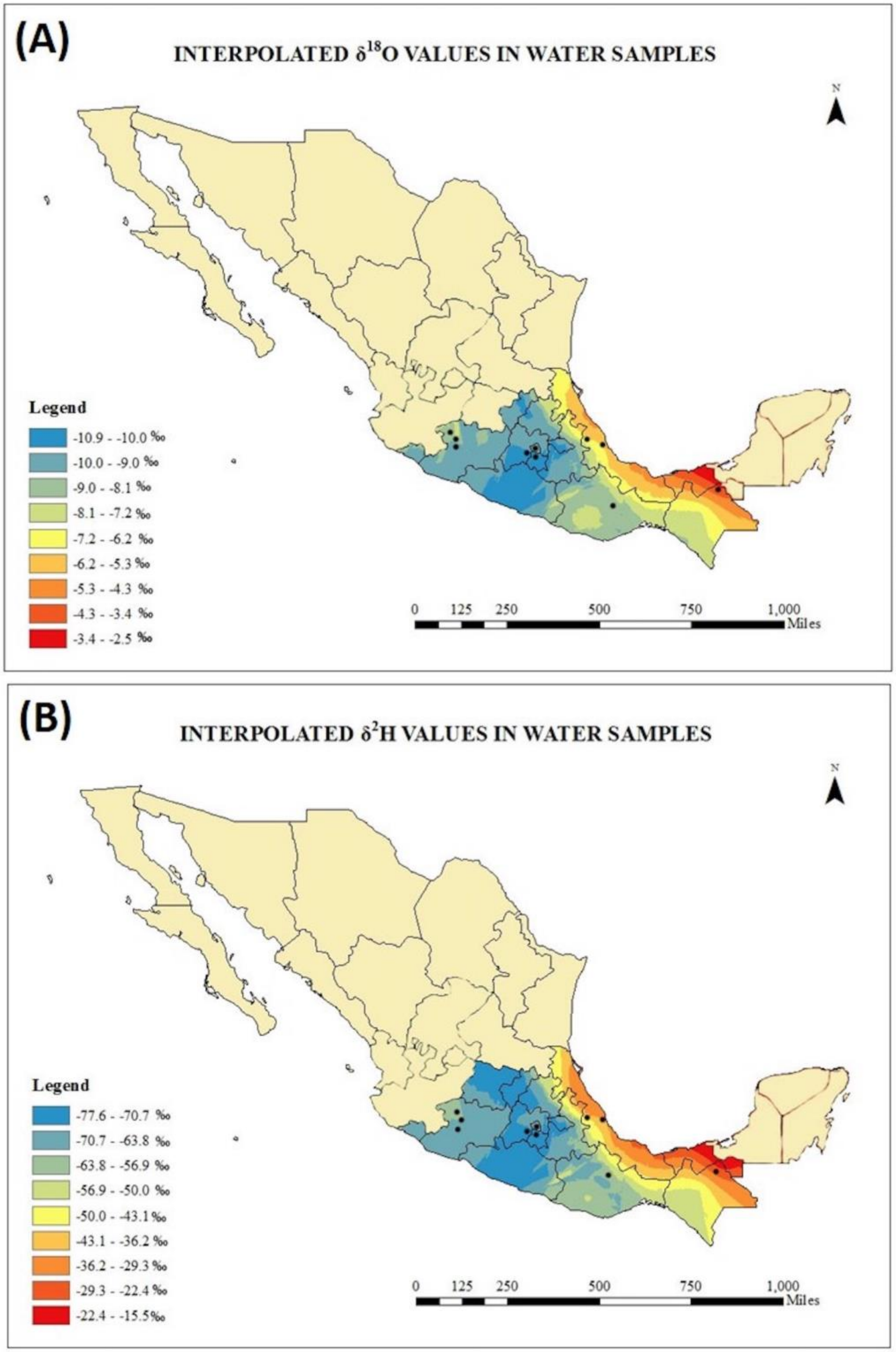
(A)
INTERPOLATED $\delta^{18}O$ VALUES IN WATER SAMPLES
N
Legend
-10.9 - -10.0 ‰
-10.0 - -9.0 ‰
-9.0 - -8.1 ‰
-8.1 - -7.2 ‰
-7.2 - -6.2 ‰
-6.2 - -5.3 ‰
-5.3 - -4.3 ‰
-4.3 - -3.4 ‰
-3.4 - -2.5 ‰
0 125 250 500 750 1,000
Miles
(B)
INTERPOLATED $\delta^{2}H$ VALUES IN WATER SAMPLES
N
Legend
-77.6 - -70.7 ‰
-70.7 - -63.8 ‰
-63.8 - -56.9 ‰
-56.9 - -50.0 ‰
-50.0 - -43.1 ‰
-43.1 - -36.2 ‰
-36.2 - -29.3 ‰
-29.3 - -22.4 ‰
-22.4 - -15.5 ‰
0 125 250 500 750 1,000
Miles

Figure 3.

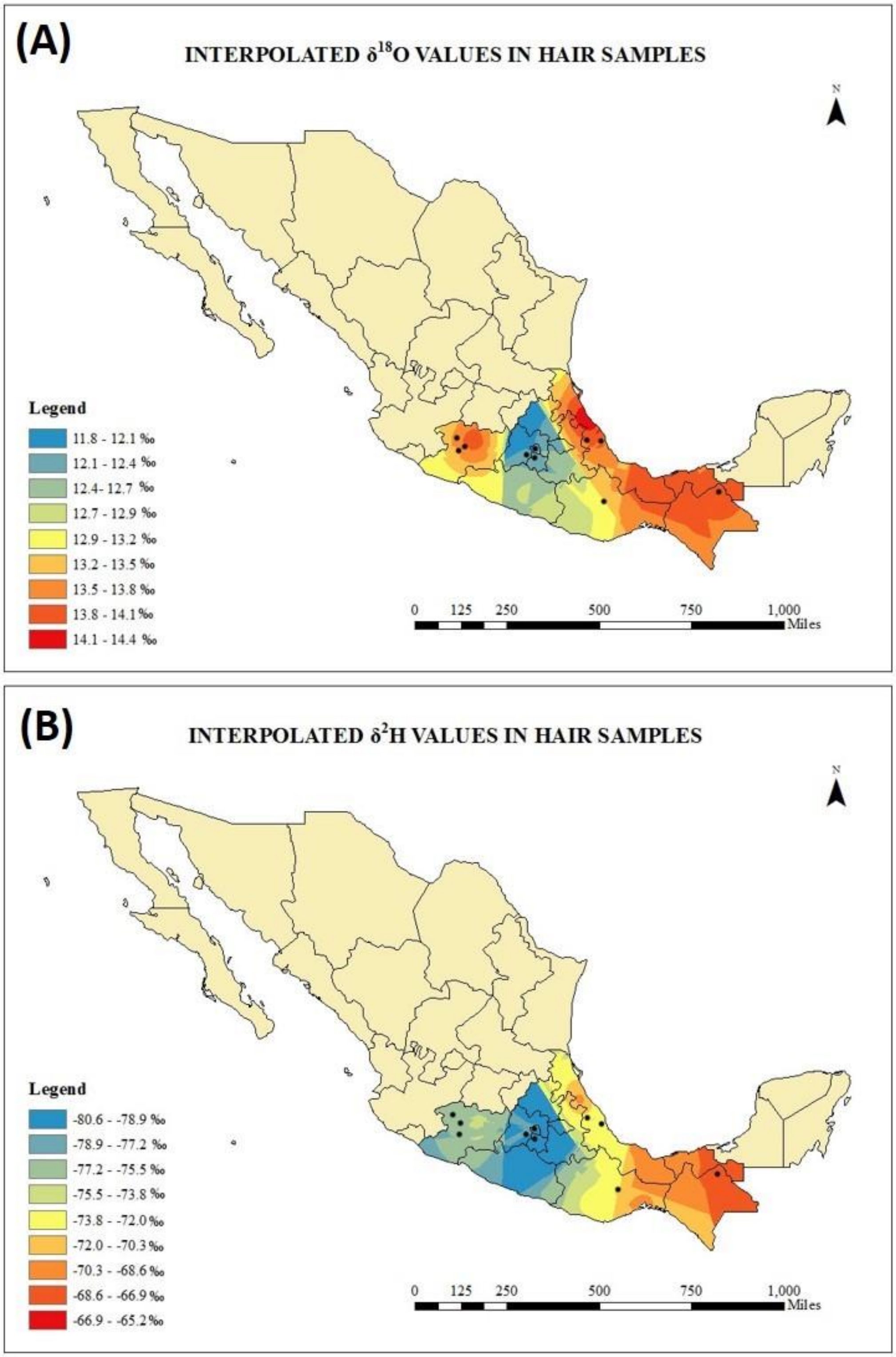
(A)
INTERPOLATED δ18O VALUES IN HAIR SAMPLES
N
Legend
11.8 - 12.1 ‰
12.1 - 12.4 ‰
12.4- 12.7 ‰
12.7 - 12.9 ‰
12.9 - 13.2 ‰
13.2 - 13.5 ‰
13.5 - 13.8 ‰
13.8 - 14.1‰
14.1 - 14.4 ‰
0 125 250 500 750 1,000
Miles
(B)
INTERPOLATED δ2H VALUES IN HAIR SAMPLES
N
Legend
-80.6 - -78.9 ‰
-78.9 - -77.2 ‰
-77.2 - -75.5 ‰
-75.5 - -73.8 ‰
-73.8 - -72.0 ‰
-72.0 - -70.3 ‰
-70.3 - -68.6 ‰
-68.6 - -66.9 ‰
-66.9 - -65.2 ‰
0 125 250 500 750 1,000
Miles

Figure 4.

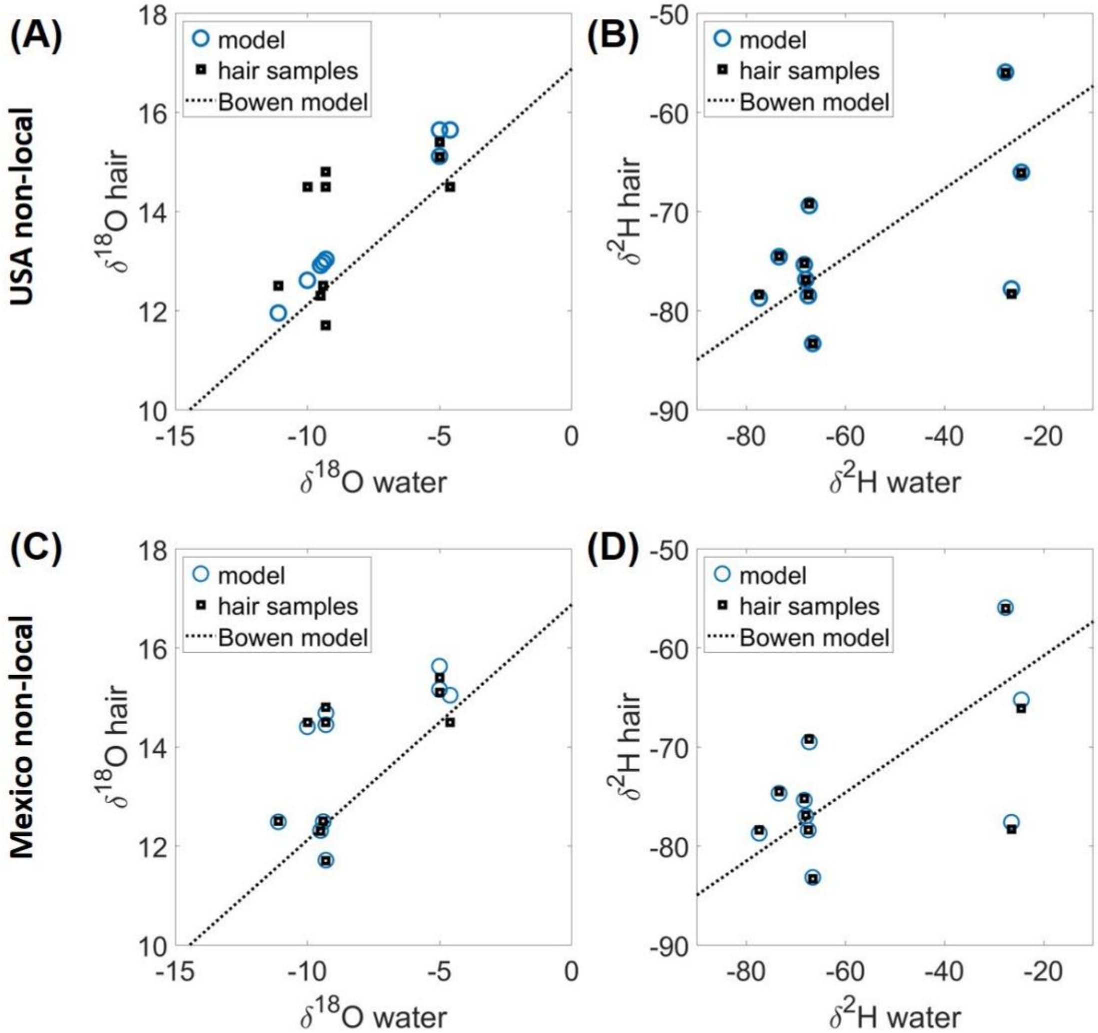

(A)
(B)
(C)
(D)
USA non-local
Mexico non-local
model
hair samples
Bowen model
δ18O hair
δ18O water
δ2H hair
δ2H water
18
16
14
12
10
-15
-10
-5
0
-50
-60
-70
-80
-90
-80
-60
-40
-20

Figure 5.

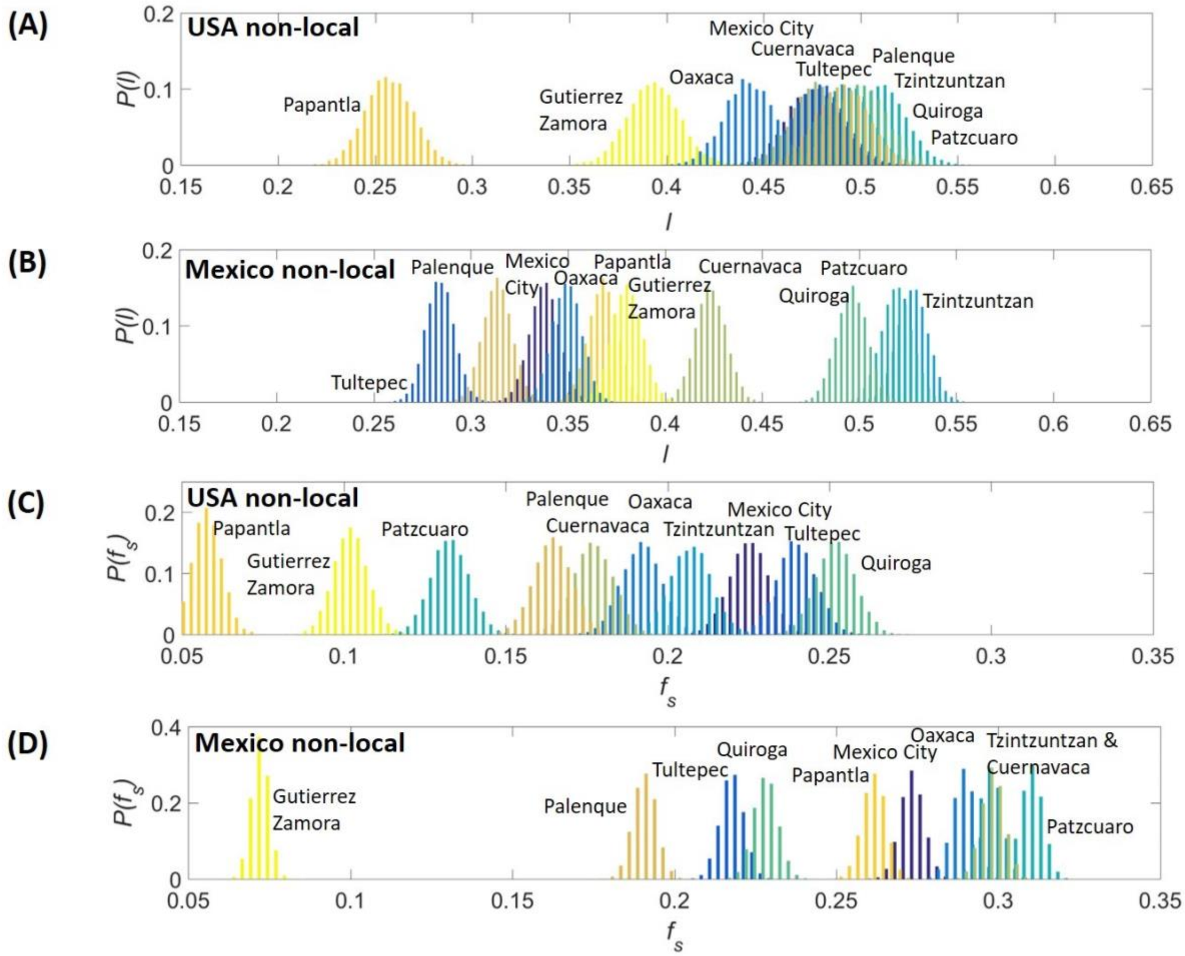

(A)
USA non-local
P(I)
Papantla
Gutierrez
Zamora
Oaxaca
Mexico City
Cuernavaca
Tultepec
Palenque
Tzintzuntzan
Quiroga
Patzcuaro
I
(B)
Mexico non-local
P(I)
Palenque
Mexico
City
Oaxaca
Papantla
Gutierrez
Zamora
Cuernavaca
Patzcuaro
Quiroga
Tzintzuntzan
Tultepec
I
(C)
USA non-local
$P(f_s)$
Papantla
Gutierrez
Zamora
Patzcuaro
Palenque
Oaxaca
Cuernavaca
Tzintzuntzan
Mexico City
Tultepec
Quiroga
f_s
(D)
Mexico non-local
$P(f_s)$
Gutierrez
Zamora
Palenque
Tultepec
Quiroga
Mexico City
Papantla
Oaxaca
Tzintzuntzan &
Cuernavaca
Patzcuaro
f_s

Figure 6.

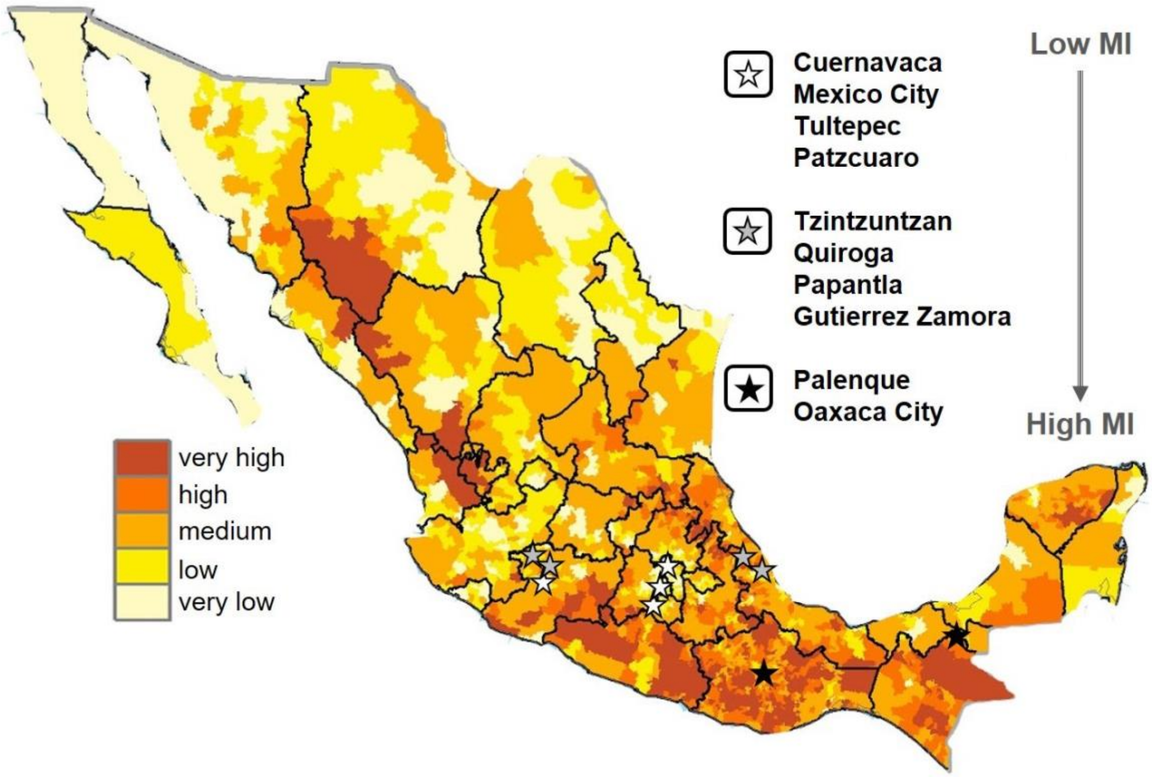
Cuernavaca
Mexico City
Tultepec
Patzcuaro
Tzintzuntzan
Quiroga
Papantla
Gutierrez Zamora
Palenque
Oaxaca City
Low MI
High MI
very high
high
medium
low
very low

Figure Captions

Figure 1. Pathway diagram showing how O and H isotopes of hair are conceptually related to the key inputs of food and water in the Ehleringer et al. (2008) and Bowen (2009) semi-mechanistic models.

Figure 2. Geographic Information System-generated maps of the predicted average (A) O isotope ratios, $\delta^{18}O$, and (B) H isotope ratios, $\delta^{2}H$, in Mexican tap water samples.

Figure 3. Geographic Information System-generated maps of the predicted average (A) O isotope ratios, $\delta^{18}O$, and (B) H isotope ratios, $\delta^{2}H$, in Mexican human hair samples.

Figure 4. Candidate model fits for Mexican paired hair/water data. (A), (B) USA non-local model. (C), (D) Mexico non-local model. Data and model predictions are shown as black square markers and blue circle markers respectively. For comparison, the model reported by Bowen et al. (2009) is also shown as a dotted line. The global values of l and f_s estimated for this linear model were estimated by Bayesian computation to be 0.24 and 0.05 respectively.

Figure 5. Credible intervals estimated for (A)&(B) l and (C)&(D) f_s in the ten locations for which paired hair/water samples were analyzed. (A)&(C) Estimates obtained using the "USA non-local" model. (B)&(D) Estimates obtained using the "Mexico non-local" model.

Figure 6. Map of Marginalization Index (MI) by municipality. Modified from Vertiz JM. Indice de marginación por entidad federativa y municipio 2010. Cons Nac POBLACIÓN, MÉXICO